Improved Method for Dispersing Clay in a Monomer or Bis(2-hydroxyl ethyl terephthalate) Before *In Situ* Polymerization of Poly(ethylene terephthalate)/ Montmorillonite Nanocomposites

Rohan Labde, Elizabeth A. Lofgren, Saleh A. Jabarin

Polymer Institute, The University of Toledo, 2801 West Bancroft Street, Mail Stop 401, Toledo, Ohio 43606-3390

Received 8 February 2011; accepted 10 September 2011
DOI 10.1002/app.35632
Published online 18 January 2012 in Wiley Online Library (wileyonlinelibrary.com).

ABSTRACT: Natural montmorillonite (MMT) clay nanomaterials were successfully dispersed in poly(ethylene terephthalate) (PET) through two new and enhanced *in situ* polymerization methods. In the case of PET/MMT nanocomposites prepared through the esterification (ES) reaction clay-addition method, unmodified MMT clays were dispersed in water and, then, the ethylene glycol monomer of PET before the preparation of bis(2-hydroxyl ethyl) terephthalate (BHET) nanocomposites, which later underwent *in situ* polymerization. For nanocomposites prepared through the polycondensation (PC) reactor method, selected amounts of clay were dispersed in ethanol, with stirring inside the reactor. A portion of crushed BHET was then added to the PC reactor, and the combined mixture was stirred to achieve dispersion. The remaining BHET was added and mixed, the ethanol was evaporated by heating, and *in situ* polymerization was initiated. Morphological analysis by X-ray diffraction and transmission electron microscopy confirmed the presence of exfoliated and intercalated clay structures in the nanocomposites prepared through both ES and PC clay-addition methods. Nanocomposites containing lower concentrations of clay showed increases in the oxygen barrier properties in comparison to values obtained for the unmodified PET. © 2012 Wiley Periodicals, Inc. J Appl Polym Sci 125: E369–E381, 2012

Key words: clay; dispersions; esterification; nanocomposites; polycondensation

INTRODUCTION

Poly(ethylene terephthalate) (PET) is a long-chain semicrystalline thermoplastic polymer that has many applications within the packaging field, particularly for use in food and beverage containers. The addition of nanoparticles to PET is expected to enhance and improve some of its commercially important properties. Polymer/clay nanocomposites are important areas of interest in both academic and industrial research laboratories as a result of their various applications.[1–5] Dennis et al.[6] gave examples of some earlier research with polymer nanocomposites,[7–9] including an *in situ* polymerization method used by Toyota, through which clay was intercalated with ε-caprolactam.

PET polymeric materials have been filled with various inorganic and/or natural compounds[10–12] to achieve increased stiffness, rigidity, and strength, greater dimensional stability, and enhanced gas barrier properties. The property improvements observed for polymers prepared as montmorillonite (MMT) clay-based nanocomposites have been due primarily to excellent dispersions of the nanoparticles in the polymers; this results in very high surface areas for contact and interactions between the filler surfaces and polymer chains.

The crystal structure of MMT clay is composed of two silicon tetrahedron sheets surrounding a single aluminum octahedron sheet. These layers are stacked and separated by van der Waals gaps. Within the crystal structure of MMT clays, some of the atoms of aluminum are replaced by magnesium, lithium, or iron by isomorphic substitution. This leads to an overall negative charge on the surface of the sheet layer, which is counterbalanced by exchangeable metal cations (e.g., sodium or calcium) residing in the interlayer spaces.[13]

Several methods have been used in an effort to obtain complete dispersion of MMT clay nanoparticles within PET polymers. These include *in situ* polymerization,[1,14,15] solution mixing,[16] and melt blending.[1,17,18] At high clay loadings, however, complete exfoliation and the subsequent desired property increases have still remained a challenge for PET researchers.[1,14–18]

Correspondence to: S. A. Jabarin (saleh.jabarin@utoledo.edu).

Contract grant sponsor: PET Industrial Research Consortium.

The primary objective of this research was to greatly improve the dispersion of natural unmodified MMT clay in a PET matrix with a new and enhanced *in situ* polymerization method. To accomplish this, appropriate solvents and pretreatment techniques were used to disperse the MMT clay in the monomer or prepolymer of PET before initiation of the polymerization reaction. For the initial step of this process, the clay was thoroughly mixed with water or ethanol to fully disperse and exfoliate the clay particles. The exfoliated clay dispersions were then combined with the other materials to replace the interlayer water with ethylene glycol (EG) or bis(2-hydroxyl ethyl) terephthalate (BHET) prepolymer. This additional dispersion step was expected to increase the penetration of the PET monomers or prepolymers into the interlayer galleries of the MMT clay platelets. The *in situ* melt-phase polymerization process was then expected to further separate the clay platelets as the PET polymer chains increased in length. The morphological, thermal, mechanical, and oxygen barrier properties of the prepared PET/clay nanocomposites were evaluated in terms of material composition and polymerization history.

EXPERIMENTAL

Materials

Polyester polymerization-grade EG was purchased from EDC Industries (Elk Grove, IL), and terephthalic acid (TPA) was donated by BP (Amoco Chemical Co., Naperville, IL). Antimony trioxide, cobalt acetate, phosphoric acid, ethanol, and tetramethylammonium hydroxide (TMAH) were purchased from Fischer Scientific (Chicago, IL). Pristine, natural, unmodified MMT clay (Cloisite Na^+) was obtained from Southern Clay Products, Inc. (Gonzales, TX) and was used without further chemical treatment.

Melt-phase polymerization

A bench-scale, melt-polymerization system (RTI Engineering Co., Ltd., Hogye-dong, Anyang Si Dongan-gu, Gyeonggi-do, South Korea) was used to prepare PET and its MMT nanocomposites. This melt-polymerization unit was equipped with an esterification (ES) reactor and a polycondensation (PC) reactor, each with a 3-L capacity. An anchor-type stirrer was used in the ES reactor, whereas the PC reactor was equipped with a helical-type stirrer for increased stirring efficiency.

The PET laboratory-scale, melt-polymerization process consisted of an ES step followed by a PC step. For the ES reaction, 560 g of EG and 1000 g of TPA (1.5 : 1 molar ratio) were reacted at 220–240°C under 1.2 kgf/cm^2 of nitrogen. Before the ES reaction was started, TMAH (100 ppm) was also added to the ES reactor to act as a diethylene glycol suppressor during polymerization. During the ES reaction, water and BHET prepolymer were produced. Water was continuously removed during the reaction by distillation, and EG was refluxed back to the reactor. The reaction was stopped when all of the EG and TPA had reacted to give a clear, colorless BHET melt. The BHET was then drained from the ES reactor, cooled, crushed, and vacuum-dried at 130°C overnight to remove residual EG and water.

The vacuum-dried BHET was transferred to the PC reactor to continue the preparation of PET. After the BHET was placed in the PC reactor, the temperature was increased, and the BHET was melted and held at 250°C for 2 h under a nitrogen environment. At this stage, 250 ppm antimony (Sb), 30 ppm cobalt (Co), and 20 ppm phosphorous (P) were placed simultaneously in the reactor (under a nitrogen flow) to act as PC additives. Before it was placed in the reactor, antimony trioxide (0.374 g) was mixed with EG (15 g) and heated up to 150°C for 2 h to form antimony glycolate, and cobalt acetate (0.166 g) was mixed with hot EG (15 g) to prepare a solution. These liquids were then added to the PC reactor, along with three drops of phosphoric acid. The PC reaction was then carried out at 275°C under high vacuum ($\sim$ 1 Torr). The polymerization reaction was stopped when the specified torque was reached for a given number of rotations per minute. The PET strands were removed under positive nitrogen pressure, quenched under cold water, and collected on a winder for evaluation and comparison to the PET nanocomposites.

As described later, the PET/clay nanocomposites were prepared by two different dispersion methods during *in situ* polymerization. The first method was designated as the ES-reactor clay-addition method (ES method). For this process, the MMT clay was dispersed in EG followed by ES and PC. The second method was designated as the PC-reactor clay-addition method (PC method). In the case of this method, the MMT clay was dispersed in previously prepared BHET followed by PC.

ES-reactor clay-addition method (ES method)

To prepare PET nanocomposites according to the ES clay-addition process, selected amounts of clay and deionized water were added to the ES reactor and stirred for 2 h at room temperature. This step was conducted to achieve complete dispersion of the clay in water at a clay/water concentration of 1% (w/w). EG was then added to the clay/water dispersion and held at 70°C with stirring until the solution was thoroughly blended. The TPA was added next (EG/TPA = 1.5 : 1 molar ratio) to the clay, water, and EG dispersion as was TMAH (100 ppm) to act as a

diethylene glycol suppressor. The combined mixture was stirred further for 2–4 h at 70°C. The reactor temperature was then raised to the ES temperature (220–240°C). As the temperature increased, water was removed by distillation. When the required temperature range was reached (as with the preparation of unmodified PET), ES was carried out to produce BHET containing clay. This BHET material was removed from the ES reactor, cooled, crushed into small chunks, and further dried overnight *in vacuo* at 130°C. The dried BHET nanocomposite containing clay was added to the PC reactor (along with the cobalt, antimony, and phosphorus PET additives), and the PC reaction was carried out at 275°C under high vacuum (~ 1 Torr). After PC was complete, nitrogen was introduced into the reactor, and the resultant PET nanocomposite was drained out as strands that were quenched in a water bath and collected on a winder. With this method, nanocomposites were prepared with the addition of clay at concentrations from 0.25 to 2 wt % in terms of the BHET prepolymer.

Method development for the preparation of BHET

In the case of the PET nanocomposites to be prepared through *in situ* polymerization in the PC reactor, the MMT clay had to be added to the BHET. An attempt was, therefore, made to disperse the pristine MMT clay directly into the melted BHET. In this case, however, the clay became suspended in the BHET, and agglomerated clay and tactoids were clearly visible with optical microscopy.

Acierno et al.[19] reported that they dispersed clay in water and transferred the water-dispersed clay into BHET, which was then dispersed in ethanol. Their mixture was stirred for 3 h at 70°C and 5 rpm. The solvents were then evaporated to yield pristine MMT modified with BHET. A variation of this method was thus chosen to disperse the MMT clay into BHET for *in situ* PC clay addition.

For the initial experiments, 50 g of pure BHET was dispersed into 800 mL of ethanol with magnetic stirring for 2 h. Clay previously dispersed in water was then added to the BHET/ethanol dispersion, and the combined mixture was stirred for 2 h. The ethanol and water were then evaporated with a hot plate at atmospheric pressure to obtain solid BHET with a 5 wt % clay dispersion in it. The BHET nanocomposite was then powdered and dried *in vacuo* for 24 h before analysis.

PC-reactor clay-addition method (PC method)

To prepare PET nanocomposites according to the PC clay-addition method, BHET was prepared by ES of EG and TPA in the ES reactor (as discussed for unmodified PET), taken out, cooled, crushed into small pieces, and vacuum-dried overnight at 130°C. Selected amounts of clay were dispersed for 2 h in ethanol (95%) at concentrations of 1% (w/w) inside the reactor with stirring. Next, 100 g of crushed BHET was added to the PC reactor, and the combined mixture was stirred for 6 h at 70°C to achieve dispersion in the slurry. The remaining crushed BHET was added to the mixture, with continuous stirring. The ethanol was evaporated by the heating of the mixture above its boiling point (78°C). The BHET and MMT clay mixture was then dried at 130°C for 15 h *in vacuo* within the PC reactor. The vacuum was released with the introduction of nitrogen, and the reactor temperature was increased to 250°C and held there for 2 h; this melted the BHET in the presence of nitrogen. The PET catalyst system was added to the PC reactor, and the PC reaction was carried out at 275°C under high vacuum (~ 1 Torr). With this PC clay-addition method, PET nanocomposites were prepared by the addition of clay at concentrations from 0.6 to 5 wt % in terms of the BHET prepolymer.

Extrusion

A laboratory-scale Brabender single-screw extruder (with a screw diameter of 19 mm, a length-to-diameter ratio of 22 : 1, and a compression ratio of 3 : 1) was used to obtain the ribbon for the preparation of sheet samples from the variously prepared pellets that had previously been vacuum-dried overnight at 140°C. The extrusion temperature was 280°C, and the screw speed was 80 rpm. The extruded ribbon was quenched with winder cooling rolls to obtain amorphous sheets of uniform thickness. The extruded sheet samples were stored at 23°C and 50% relative humidity before mechanical property and permeability evaluations.

Characterization

A wide-angle Rigaku Ultima III multipurpose X-ray diffraction (XRD) system (The Woodlands, TX) was used to determine changes in the basal spacings of the prepared clays and nanocomposite samples. Instrument specifications included a nickel filter, Kα (1.541 Å), and a scanning speed of 0.4°/min in the range $2\theta = 1.5$–9° at 45 kV and 40 mA.

Morphological analyses were carried out with a Hitachi HD-2300A scanning transmission electron microscope (Tokyo, Japan) with samples prepared with an LKB Nova ultramicrotome (Broma, Sweden). Before being microtomed, the polymer nanocomposite samples were embedded in epoxy resin. After the epoxy resin was cured, ultrathin sections of the nanocomposite samples were cut with a glass knife. The sample slicing speed was 1 mm/s. These samples had thicknesses in the range 50–100 nm.

The microtomed sections were collected on 300-mesh copper grids and subsequently dried. During transmission electron microscopy (TEM) analysis, the film samples were mounted on an electron gun and inserted into the vacuum chamber, which was set at 10^{-7} Torr of pressure. These ultrathin samples were then analyzed by an HD-2300A TEM instrument (Tokyo, Japan) at a 200-kV accelerating voltage.

To determine their gross levels of dispersion in various liquids, the samples were visually examined on glass slides with the use of a Zeiss transmission optical microscope (Oberkochen/Wuertt., West Germany) at a magnification of about 60×.

The sample melt viscosities were measured with a parallel-plate Rheometric Scientific (RDA III) dynamic analyzer (Piscataway, NJ) with a frequency sweep from 1 to 100 rad/s and a gap between the plates of 1 mm. Vacuum-dried pellet samples were evaluated at a temperature of 280°C in the presence of a nitrogen purge to prevent oxidation. The melt viscosity values taken at 10 rad/s were converted to PET equivalent intrinsic viscosity values according to the method described by Tharmapuram and Jabarin.[20]

Thermal properties of the PET and nanocomposites were monitored with a PerkinElmer (DSC-7) differential scanning calorimeter (Shelton, CT) calibrated with indium and zinc standards. Samples of about 10 mg were heated and cooled at the rates specified in a nitrogen environment to prevent oxidative degradation. The crystallization and melting characteristics and glass-transition temperatures (T_g's) were evaluated.

The tensile modulus, tensile strength, and maximum strain were measured with an Instron 4400R universal testing system (Norwood, MA) according to ASTM D 638 with type I specimens. The dog-bone-shaped samples prepared for this study were die-cut from the sheets at room temperature. Each specimen had a 50.8-mm (2-in.) gage length and was 12.7 mm (0.5 in.) wide at its narrow portion. The thickness of each specimen was measured with a micrometer and found to range from 0.025 to 0.089 mm (1–3.5 mil). All samples were stored at 50% relative humidity and 23°C for at least 48 h before being evaluated. The tensile properties were measured at a crosshead speed of 50.8 mm/min (2 in/min) at room temperature.

Oxygen permeability analyses of the PET nanocomposite films were performed with a MoCon OxTran 1050 permeability tester (Minneapolis, MN) according to ASTM D 3985. These measurements were carried out at 1 atm, 23°C, and 50% relative humidity. Before being evaluated, the films were cut to fit the 12-cm^2 area of the circular test holder of the permeation cell. All samples were conditioned for at least 12 h in the apparatus before being evaluated. During measurement, the permeation cell was flushed with oxygen gas on one side and nitrogen carrier gas on the other. The flow rates of the oxygen and nitrogen were each maintained at 25 cm^3/min.

RESULTS AND DISCUSSION

The *in situ* polymerization method chosen for the preparation of PET/clay nanocomposites requires that the MMT clay be completely dispersed in the PET monomers or prepolymers before and during the *in situ* polymerization process. As a result, preliminary investigations and experiments have been conducted to develop a method that could achieve those goals. Jacobson[21] showed that pristine MMT natural clay could be easily dispersed and exfoliated in water. Sun et al.[22] exchanged water-dispersed clay into acetone by a centrifugation and dispersion method so that it could be transferred to a hydrophobic epoxy polymer. In addition, Wang et al.[23] prepared well-exfoliated clay/epoxy nanocomposites using a process in which the clay was first dispersed and exfoliated in water. It was then treated with acetone and chemically modified before it was mixed with epoxy to obtain epoxy nanocomposites. In a similar manner, the MMT clay used for these experiments was dispersed in water or ethanol with various techniques.

During the preliminary experiments, the MMT clay was dispersed in water first by sonification and also with magnetic stirring. It was concluded that the clay particles were swollen and better dispersed in the water when magnetic stirring was used, and the resulting mixture was held in suspension for several hours. With the use of transmission optical microscopy at 60× magnification, it could be seen that clay tactoids (which appeared in the dispersions as black spots) were suspended in water after sonification; however, after magnetic stirring, the dispersions appeared to be clear, without any visible clay tactoids. In separate experiments, the clay was added directly into EG. Even though EG is hydrophilic in nature, the clay did not completely disperse in it and was observed to form a suspension in the mixture.

EG is miscible in water; therefore, additional clay dispersions were first prepared in water, and the water-exfoliated clay was then combined with EG. As EG has a boiling point 197°C, water was removed by the heating of the dispersion above 100°C. It was observed that as long as there was sufficient water present, the clay platelets remained well dispersed in the solution. As the water percentage in the mixture was reduced, however, the agglomeration of clay in EG occurred, and the mixture became more viscous. This may have occurred because when clay is exfoliated, it requires a certain volume of water to remain exfoliated. As water was removed from the mixture, the clay platelets in the dispersion did not have enough volume to remain exfoliated, and this caused the mixture to become

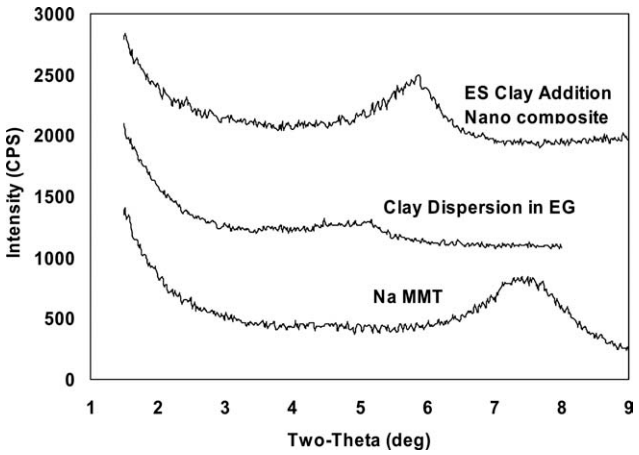

Figure 1 XRD patterns of MMT clay, an EG–MMT clay dispersion, and a 0.5 wt % clay ES addition PET/MMT nanocomposite.

viscous.[24] Figure 1 gives the XRD patterns obtained for MMT clay alone and clay dispersed as a viscous gel in EG. It can be seen that a small peak existed at a diffraction angle of 5.45° for the clay in EG. This shift from the 7.4° value seen for pure clay indicated that some of the EG entered the registers between the clay platelets and caused them to be more separated or intercalated. The presence of this small peak, however, indicated that all of the clay was not exfoliated in the EG because totally exfoliated clay would not give any XRD pattern. Other researchers have also reported that similar EG–clay mixtures have given intercalated XRD patterns exhibiting a diffraction peak at $2\theta = 5.6°$.[25,26]

Clay addition for the ES reaction (ES addition)

A series of ES addition PET nanocomposites were prepared, as described in the Experimental section. Figure 1 includes the XRD pattern of a 0.5% clay/PET nanocomposite prepared through ES *in situ* polymerization in addition to MMT clay alone and clay dispersed in EG. The 2θ diffraction angle of 5.7° obtained for the PET nanocomposite was lower than the 7.4° value of the pure clay. This peak shift to a lower angle indicated intercalation of the polymer nanocomposite chains into the interlayer spaces of the clay platelets and showed that interlayer spaces increased from 1.12 nm for the MMT clay to 1.5 nm for the nanocomposite. The relatively large size of the peak also indicated that intercalation rather than exfoliation was the dominant condition for the clay. As previously discussed, the clay was not completely exfoliated during dispersion in EG. The XRD spectrum given in Figure 1 indicates that for some of the clay particles, no further exfoliation occurred during the ES and PC reactions, which may also have resulted in some additional agglomeration of the clay.

Clay addition for the PC reaction (PC addition)

MMT clay had to be combined with BHET for PET nanocomposites to be prepared through *in situ* polymerization in the PC reactor. During our preliminary work (Experimental section), a technique was developed for this purpose. Figure 2 shows a wide-angle X-ray pattern obtained for the prepared, dried BHET–clay powder. As shown, there was a peak at $2\theta = 4.45°$, which was equivalent to an interlayer spacing of $d = 1.96$ nm. Because the MMT platelets (with a diffraction peak at $2\theta = 7.3°$) exhibited interlayer spacing values of $d = 1.12$ nm, we concluded that BHET became intercalated in the galleries of the MMT clay platelets and increased the basal spacing of the clay by 0.84 nm. To verify that the 4.45° diffraction peak resulted from intercalation and was not from BHET, an XRD pattern of pure BHET was obtained and was found to have no diffraction peaks up to $2\theta = 9°$. It was expected that during the polymerization of BHET that had been intercalated within the clay platelets, the growth of the polymer chains would further separate the interlayer spacing between the platelets and result in a better dispersion of the MMT clay within the PET matrix.

The PC clay-addition method, described in the Experimental section, was used to prepare PET nanocomposites containing from 0.6 to 5 wt % MMT clay. Figure 2 shows an XRD pattern for the 0.6 wt % clay nanocomposite. As can be seen by a comparison to the patterns obtained for the pure clay and the BHET–clay dispersion, the PC reaction further separated the clay platelets as the polymerization reaction progressed. The peaks that were obtained for both the BHET clay powder and the PC addition PET nanocomposite were shifted from the $2\theta = 7.3$ ($d = 1.12$ nm) value of the pure clay. Their patterns were reduced to $2\theta = 4.4°$ ($d = 1.96$ nm). The intensity of the peak that was obtained for the PET nanocomposite was also reduced significantly from that of the BHET clay powder. The peak shift of $2\theta = 4.4°$ and the reduction in intensity for the PET nanocomposite clearly showed an increase in the interlayer spacing of the MMT platelets as a result of the intercalation of MMT by the PET polymer chains.

TEM

TEM was used to supplement the results obtained through morphological analysis of the PET nanocomposites by XRD. Figure 3 shows TEM images of ES and PC prepared PET nanocomposites. The dark lines in the figure represent individual MMT clay sheets having 1-nm thicknesses and aspect ratios of about 100 nm. The gray areas between and surrounding the dark lines represent the volume occupied by the polymer matrix. Figure 3(a) is the TEM

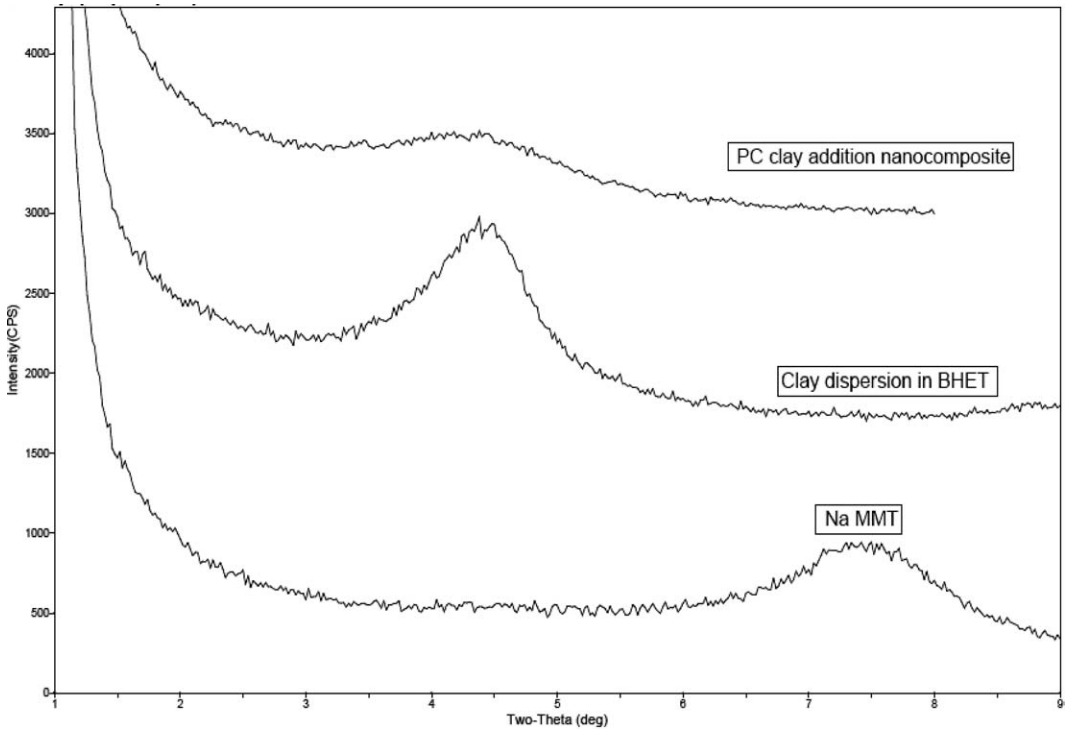

Figure 2 XRD patterns of MMT clay, clay–BHET powder, and a 0.6 wt % clay PC addition PET/MMT nanocomposite.

image of the 0.5 wt % clay ES addition nanocomposite. It can be seen that the layer structure of MMT clay was more randomly dispersed for this ES clay-addition nanocomposite than that seen for the 0.6 wt % clay PC addition nanocomposites, which is shown in Figure 3(b). Single and double black lines were seen for the ES clay-addition nanocomposite, as shown in Figure 3(a). These represented the clay platelets separated from the layered structure and dispersed in the PET matrix. This verified that good dispersion of clay platelets was achieved in the PET matrix. Agglomerated clay particles were also detected for both ES and PC prepared nanocomposites. For the PC clay-addition nanocomposite [Fig. 3(b)], the TEM image shows that most of the MMT clay layers were randomly distributed with a face-to-face stacked style. They also show increased interlayer spaces between the clay layers, in which PET chains were intercalated; this was consistent with the XRD results. The results obtained with TEM and XRD indicated that both ES and PC clay-addition methods produced PET nanostructures in which the MMT clay platelets were partially intercalated and partially exfoliated by the PET matrix.

Evaluations and comparisons of the nanocomposite physical properties

The properties of the nanocomposites prepared by each of the *in situ* polymerization methods were compared in regard to the levels of clay added and the reaction type (ES vs PC). Because the times of their PC reactions were controlled by the monitoring of the torque applied for stirring during melt polymerization, they exhibited similar melt viscosities at 280°C. These values were converted[20] to PET equivalent intrinsic viscosity values and were within the range from 0.65 to 0.71 dL/g.

The thermal properties of the various nanocomposites were monitored with differential scanning calorimetry to determine whether the presence of the clay significantly altered their major transitions. Resin samples were finely ground and vacuum-dried overnight at 130°C before analysis. All samples (8–13 mg) were heated to 300°C to remove their thermal history and quenched to 40°C before comparison in terms of their T_g, crystallization, and melting behaviors. The various transitions observed during reheating of the previously melted and quenched samples at 10°C/min are given in Figure 4. As shown, T_g (79°C) and the melting peak temperature (T_m; 248°C) of most of the nanocomposites remained nearly the same as those of neat PET. Differences, however, were observed in their crystallization behaviors. The ES clay-addition nanocomposites [Fig. 4(a)] showed cold crystallization peaks at low clay loading, but as the clay content increased, the sizes of the peaks diminished. Thermograms for the PC clay-addition nanocomposites [Fig. 4(b)] showed very little, if any, cold crystallization during reheating. The absence of a cold crystallization exotherm during the reheating of a PET sample that exhibits a melting endotherm indicates that crystallization had previously

Figure 3 TEM images of PET/MMT nanocomposites prepared through (a) 0.5 wt % clay ES addition and (b) 0.6 wt % clay PC addition.

occurred during cooling. This can occur when a sample has a very rapid rate of crystallization that exceeds its cooling rate.

As seen in Figure 4, the ES clay-addition nanocomposites exhibited cold crystallization peaks at low clay loading; however, as the clay contents increased, the sizes of the exotherms diminished. Most of the PC clay-addition nanocomposites appeared to have crystallized during quenching, as their thermograms did not show significant levels of cold crystallization. The reduction or absence of cold crystallization indicated that addition of higher ES clay contents and most PC clay contents resulted in the agglomeration of clay, which acted as a heterogeneous nucleating agent and caused the nanocomposite to crystallize during quenching.[27]

To evaluate the tendency of the nanocomposites to crystallize when being cooled from the melt, cooling thermograms were recorded for selected samples. Figure 5(a,b) gives the cooling results obtained for ES prepared 0.5 and 2% clay nanocomposites [Fig. 5(c)] and a PC prepared 2% clay nanocomposite. As these samples were cooled from the melt at faster cooling rates, crystallization was delayed, but the samples still showed substantial crystallization. In addition, samples with higher clay contents were seen to crystallize at higher temperatures, with those prepared in the PC reactor crystallizing most readily. From these results, we concluded that levels of clay agglomeration in the polymer increased at higher clay contents, and these agglomerated clay particles acted as nucleating agents; this resulted in increased rates of crystallization and, thus, higher temperature crystallization peaks.[27]

It was also observed that at each cooling rate, the crystallization peak temperatures (T_c's) recorded for the PC clay-addition nanocomposites were slightly higher than those of equivalent ES clay-addition nanocomposites; this indicated faster rates of crystallization. From this, we concluded that the clay was better dispersed in the polymer materials prepared by the ES clay-addition method and at low clay contents. Others observed that when clay remains intercalated and agglomerated in a polymer material, it acts as a nucleating agent and increases the rate of crystallization; however, when the clay is well exfoliated, it has little effect on the crystallization rate.[27]

Further crystallization evaluations and comparisons of the ES- and PC-reactor nanocomposite samples of each composition were obtained by their cooling from the melt at 10°C/min with DSC. The effects of different clay concentrations on these nanocomposites are shown in Figure 6. The major transitions recorded for these materials are summarized in Table I, which also includes the melting transitions obtained during reheating of the crystallized materials at 10°C/min. For comparison, the table gives the crystallization onset temperature (T_{co}), or the temperature at which the thermograph initially departs from the baseline, T_c, the heat of crystallization (ΔH_c), the melting onset temperature (T_{mo}), T_m, and the heat of fusion (ΔH_f). All of the samples exhibited similar T_{mo} and T_m values, with their ΔH_f values following trends similar to those obtained during crystallization.

As shown in Figure 6, crystallization peaks recorded for all of the samples were fairly symmetrical in nature. Because this was the case, the crystallization half-times ($t_{1/2}$'s) obtained for these nonisothermal cooling curves could be calculated with the following equation:[28,29]

$$t_{1/2} = (T_{co} - T_c)/\Theta \quad (1)$$

where $t_{1/2}$ represents the time required for each PET nanocomposite to reach 50% of its total degree of crystallinity, T_c is the exotherm peak temperature, and Θ is the cooling rate.

As shown on Table I, all of the PET/MMT nanocomposites exhibited shorter $t_{1/2}$ values than that of unmodified PET; this indicated that the MMT clay played a nucleating role during crystallization. At

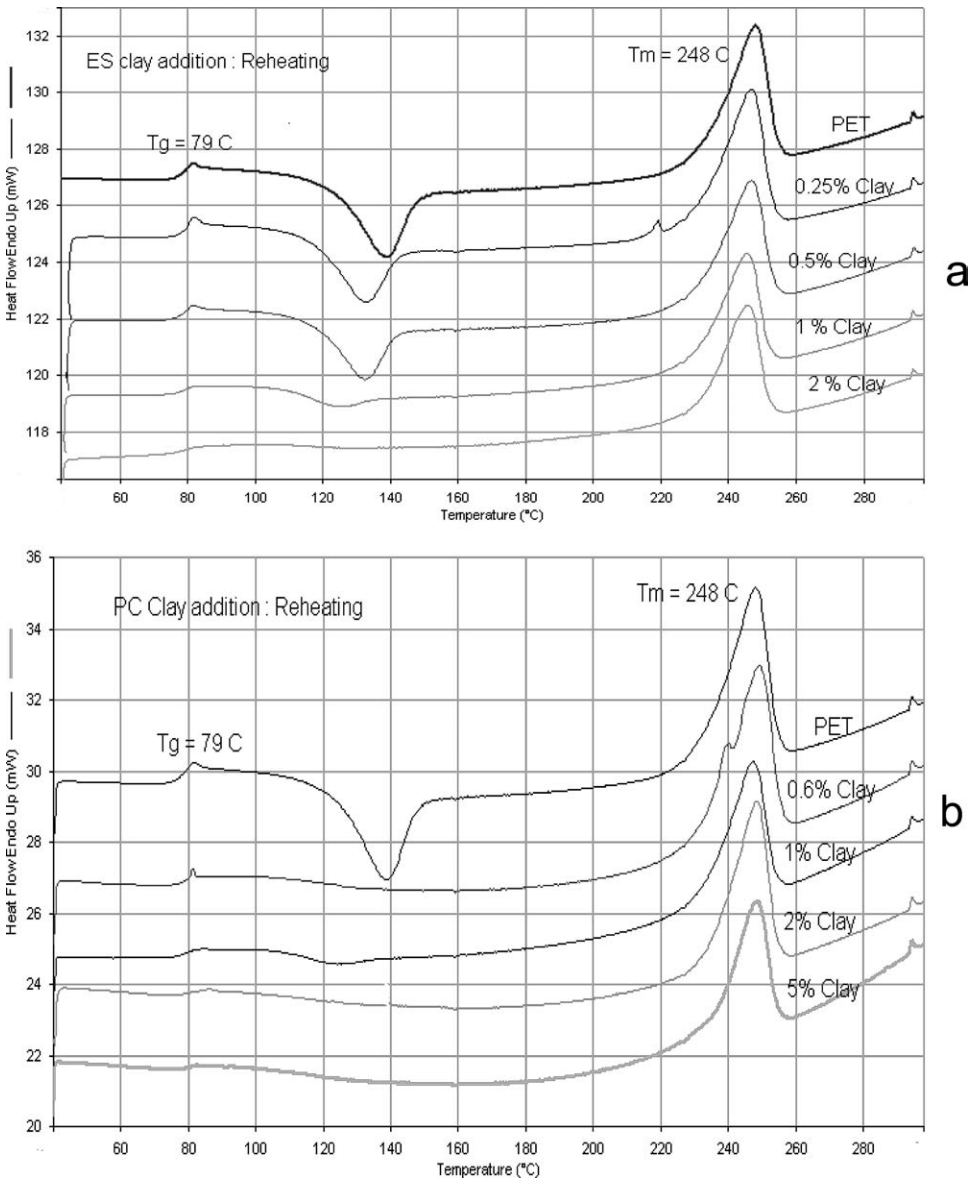

Figure 4 DSC thermograms showing reheating at 10°C/min of quenched PET and various weight percentages of clay (a) ES and (b) PC addition PET/MMT nanocomposites.

lower clay loadings, the $t_{1/2}$ values of ES clay-addition nanocomposites were more similar to that of PET; this indicated that at lower levels, the clay in these samples had less effect on the crystallization rate. All of the PC clay-addition nanocomposites had slightly smaller $t_{1/2}$ values than those prepared through the ES clay-addition method; this indicated a stronger nucleating effect by clay added to BHET in the PC reactor. The ΔH_c values measured for the nanocomposites prepared by both the ES and PC addition methods were slightly larger than that of PET and increased with increasing clay content. Increases in ΔH_c measured for the ES clay-addition method nanocomposites, however, were slightly smaller than those of nanocomposites prepared through the PC clay-addition method.

The T_{co} and T_c values of the nanocomposites were higher than those of neat PET; this indicated more rapid rates of crystallization. Relative differences in the crystallization rates could be further compared in terms of ΔH_c divided by the time from the onset to the completion of crystallization. As shown in Table I, the nanocomposites prepared through the PC clay-addition method showed slight increases in these values with increased clay contents. The values obtained for ES prepared samples with low clay loadings, however, were close to that of neat PET; this indicated that ES clay addition did not increase the crystallization rates as much as the PC clay-addition method did.

Mechanical properties of the neat PET and PET/MMT nanocomposites

The tensile mechanical properties of the PET nanocomposites (obtained from the stress–strain curves

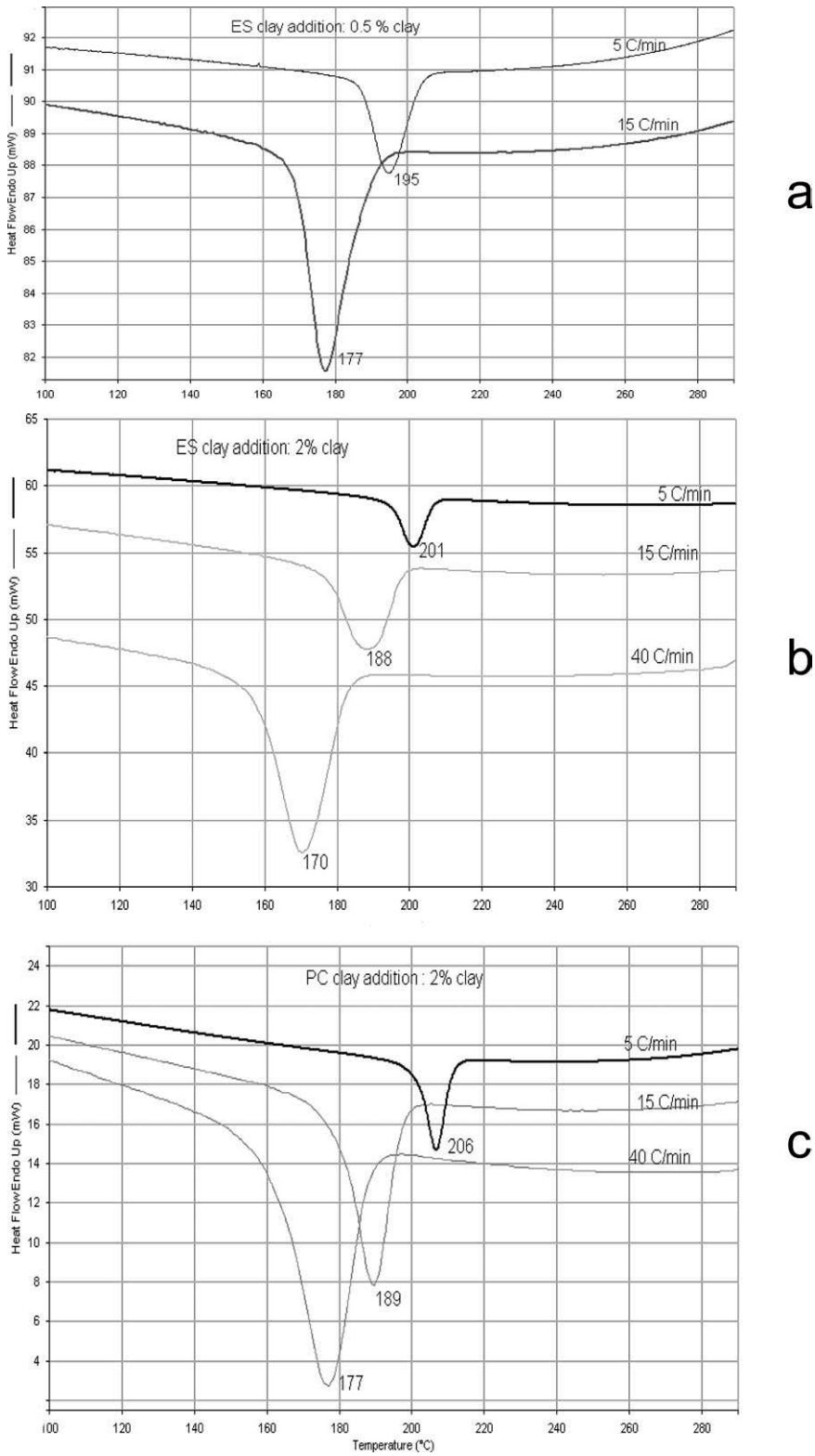

Figure 5 DSC thermograms for the ES and PC prepared PET/MMT nanocomposites with different cooling rates of (a) 0.5 wt % clay ES addition nanocomposites, (b) 2 wt % clay ES addition nanocomposites, and (c) 2 wt % clay PC addition nanocomposites.

of the Instron tester) are summarized in Table II. It can be seen that the PET nanocomposites prepared with both the ES and PC methods generally exhibited higher yield strength and modulus values than the unmodified PET. The nanocomposites prepared through ES clay addition with low clay loadings showed the greatest overall improvements in their mechanical properties.

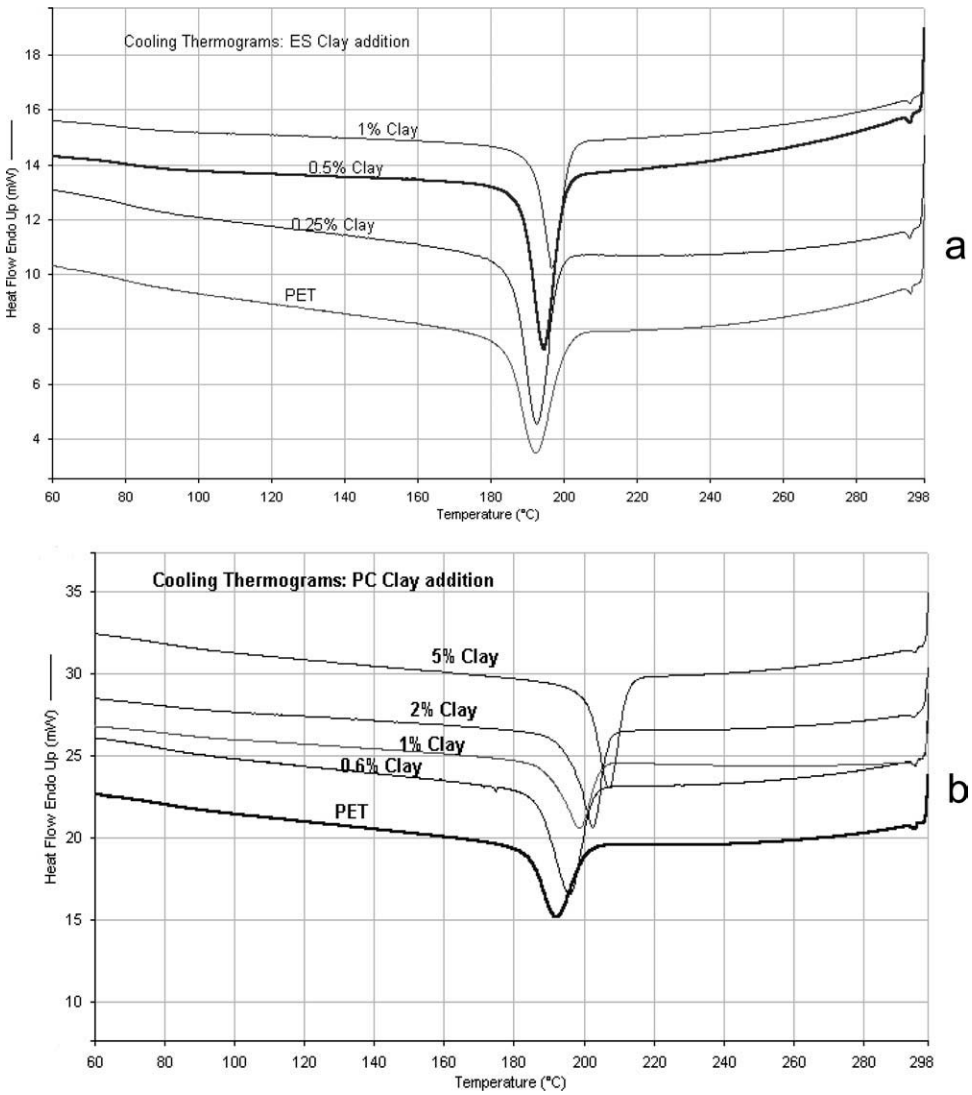

Figure 6 DSC thermograms of various PET/MMT nanocomposites cooled from 300 to 40°C at 10°C/min of various weight percentages of clay (a) ES and (b) PC addition nanocomposites.

As shown in Table II, the ES addition method nanocomposite with 0.5 wt % clay exhibited the maximum increase in the tensile strength (84%) compared to neat PET. It could be observed that as the clay levels increased for the ES addition samples, their tensile strengths increased up to 0.5 wt % clay,

TABLE I
Thermal Data Collected from the DSC Thermograms of the Unmodified PET and ES and PC Clay-Addition PET/MMT Nanocomposites

	Cooling at 10°C/min[a]					Reheating after crystallization		
Clay in PET (wt %)	T_{co} (°C)	T_c (°C)	$t_{1/2}$ (min)	ΔH_c (J/g)	ΔH_c/time (J/g/s)	T_{mo} (°C)	T_m (°C)	ΔH_f (J/g)
0	207	192	1.5	32	0.18	207	248	34
ES clay addition								
0.25	206	193	1.4	32	0.19	206	247	34
0.50	207	194	1.4	34	0.20	204	248	36
1.00	206	196	1.2	35	0.25	206	247	36
PC clay addition								
0.60	207	196	1.1	36	0.28	206	248	38
1.00	210	198	1.2	36	0.26	207	248	37
2.00	213	202	1.1	38	0.29	206	248	39
5.00	217	207	1.0	39	0.32	207	247	39

[a] Cooling from 300 to 40°C.

TABLE II
Tensile Mechanical Properties of the Unmodified PET and PET/MMT Nanocomposites

Composition of clay in PET (wt %)	Strength at yield		Tensile modulus		Elongation at break (%)
	MPa	Increase (%)	MPa	Increase (%)	
0	49 (2.7)	0	960 (55)	0	350 (50)
ES clay addition					
0.25	70 (4.1)	43	1470 (50)	53	625 (80)
0.50	90 (5.2)	84	1840 (140)	92	530 (56)
1.00	71 (3.7)	45	1340 (120)	40	Brittle[a]
2.00	51 (7.2)	4	1105 (90)	15	Brittle[a]
PC clay addition					
0.6	70 (2.1)	43	1160 (80)	21	540 (46)
1.00	65 (1.6)	32	1080 (40)	13	Brittle[a]
2.00	68 (2.9)	38	1200 (52)	25	Brittle[a]
5.00	38 (2.4)	−22	1005 (60)	5	Brittle[a]

Standard deviations are given in parentheses.
[a] More than 80% of the samples broke without elongation.

with further increases in clay contents resulting in decreased tensile strengths. In the case of samples prepared through the PC clay-addition method, the maximum increase in tensile strength was observed for 0.6 wt % clay addition (43%), with additional clay loadings giving decreased tensile strengths.

Similar trends were observed for the tensile modulus values measured for the PET nanocomposites. Those prepared by the ES addition method with 0.5 wt % clay showed a 92% increase in the tensile modulus values, whereas all other nanocomposites exhibited lower levels of improvement. The mechanical property improvements observed for the PET/MMT nanocomposites were thought to have occurred because the intercalation and exfoliation of the clay nanoparticles in the polymer matrix resulted in the availability of high surface areas of the clay platelets for interaction with the PET chains and for interfacial adhesion and ionic bond formation.[30] Clays are very rigid and have a very high modulus[31] compared to a polymer matrix. When force is applied to a PET nanocomposite, most of the force is thought to be transferred to the clay particles. This would give a nanocomposite greater stiffness and higher tensile strength and modulus values compared to unmodified PET. Because the mobilities of the polymer chains would also be reduced close to the surface of the clay platelets, this would also result in increased modulus values.[32,33]

Nanocomposites prepared through both the ES and PC methods showed similar mechanical properties at higher clay loadings. The nanocomposites containing 1% or more MMT showed extreme brittleness, and it was difficult to measure their mechanical properties. The elongation at break values illustrated this trend. For low clay contents, these values were observed to increase in comparison to that of unmodified PET; however, at higher loadings, the samples all exhibited brittle failure during extension. This may have occurred partially because no organic modifier was used to increase the compatibility between the PET and MMT, and at a higher clay loadings, the natural clay agglomerated more easily. It has been reported that polymer nanocomposites prepared from organically modified clay showed better tensile properties than nanocomposites prepared from natural clay (MMT) at higher clay loadings.[16,34–37]

Changes in the crystallization behaviors observed for the nanocomposites indicated that as the clay concentration increased, the agglomeration of clay in the PET matrix increased. This agglomeration and possible microvoid formation could have also resulted in the increases in stiffness observed through mechanical property evaluations. The results indicate that among important factors contributing to the enhancement of the mechanical properties of the PET/MMT nanocomposites was the degree of dispersion and exfoliation of the clay platelets in the polymer matrix.[34,36]

Oxygen permeability testing of the PET/MMT nanocomposites

The oxygen (O_2) permeability values obtained for unmodified PET and the PET/MMT nanocomposites are compared in Table III. As can be seen, the ES 0.5 wt % clay-addition nanocomposite exhibited a permeability that was 36% lower than that of the neat PET. The nanocomposite prepared by PC addition with 0.6% clay showed a slightly lower improvement at 31%. Although these decreases in permeability were small, they were significant. One can also see that as the levels of clay loading were increased, no further decreases in the O_2 permeability were obtained. The presence of well-dispersed clay in a PET matrix is expected to produce a reduction in the permeability because the clay

TABLE III
Experimental Oxygen Permeability Values of the Unmodified PET and PET/MMT Nanocomposites

Polymer nanocomposite	Clay (wt %)	O_2 permeability (ccmil 100 in.$^{-2}$ day^{-1} atm^{-1})	Average decrease in O_2 permeability (%)
PET	0	8.4 (0.55)	—
ES clay addition	0.5	5.4 (0.26)	36
ES clay addition	2.0	5.8 (0.40)	29
PC clay addition	0.6	5.7 (0.30)	31
PC clay addition	2.0	6.3 (0.50)	25

Standard deviations are given in parentheses.

platelets create an increased tortuous path for the O_2 permeant molecules.[1,38] The observed trend in the barrier properties with increased clay loading was similar to that of the mechanical properties. The lack of improvement with increased clay loading probably resulted from agglomeration of the MMT clay in the polymer matrix in the case of both the ES and PC clay-addition methods.

CONCLUSIONS

Morphological analysis by XRD and TEM confirmed the presence of exfoliated and intercalated clay structures in nanocomposites prepared through both ES and PC clay-addition methods. TEM images showed an enhanced separation of clay platelets in the PET matrix for a 0.5% clay nanocomposite sample prepared through the ES clay-addition method.

Although there were no significant changes in T_g and T_m of the nanocomposites, the crystallization rates were found to increase for samples cooled from the melt. Greater increases were observed at higher clay loadings, with the PC addition nanocomposites showing a slightly greater tendency to crystallize than those prepared through the ES addition method. These increased tendencies to crystallize probably resulted from the agglomeration of clay in the polymer matrices and indicated that PET/MMT nanocomposites prepared by the ES clay-addition method had a slightly better dispersion of clay platelets within the PET matrix in comparison to the PC clay-addition nanocomposites.

The tensile strength and tensile modulus properties of the nanocomposites increased at low clay loadings compared to equivalent values of PET. As the clay percentage increased, however, substantial decreases in the mechanical properties were observed because of the agglomeration of clay.

Oxygen barrier properties of a 0.5 wt % clay ES addition nanocomposite material were found to increase 36% over those of the unmodified PET, whereas a similar 0.6% clay PC prepared material showed a barrier increase of 31%. The addition of higher levels of clay gave reduced barrier improvements for both the ES and PC prepared materials.

The morphological, thermal, mechanical, and permeation analyses showed that PET/MMT nanocomposites prepared through both the ES and PC clay-addition methods showed good dispersion of the clay at low MMT concentrations. At higher clay loadings, however, nanocomposites prepared through both methods exhibited higher levels of clay agglomeration. This was observed in terms of their diminished property improvements. More work is needed to achieve greater PET/MMT compatibility and to improve the dispersion of clay nanoparticles in the PET matrix, particularly at higher clay loadings.

References

1. Kim, S.-G. Ph.D. Thesis, Polymer Institute, University of Toledo, 2007.
2. Jabarin, S. A. Polymeric Materials Encyclopedia; CRC: Boca Raton, FL, 1996; Vol. 8, pp 6078, 6091.
3. PET Packaging Technology; Brooks, D. W., Giles, G. A., Eds.; Sheffield Academic: Sheffield, United Kingdom, 2002; pp 3, 16.
4. Mahajan, K. Ph.D. Thesis, Polymer Institute, University of Toledo, 2010.
5. Legras, R.; Belly, C.; Daumerie, J. M.; Dekoninck, J. M.; Zichy, V. Polymer 1984, 25, 835.
6. Dennis, H. R.; Hunter, D. L.; Chang, D.; Kim, S.; White, J. L.; Cho, J. W.; Paul, D. R. Polymer 2001, 42, 9513.
7. Kojima, Y.; Usuki, A.; Kawasumi, M.; Okada, A.; Kurauchi, T.; Kamigaito, O. J Appl Polym Sci 1993, 49, 1259.
8. Kojima, Y.; Usuki, A.; Kawasumi, M.; Okada, A.; Kurauchi, T.; Kamigaito, O. J Appl Polym Sci 1993, 31, 983.
9. Yano, K.; Usuki, A.; Okada, A.; Kurauchi, T.; Kamigaito, O. J Polym Sci Part A: Polym Chem 1993, 31, 2493.
10. Chang, J.-H.; Mun, M. K. Polym Int 2007, 56, 57.
11. Pegortti, A.; Penati, A. Polymer 2004, 45, 7995.
12. Lee, H.-J.; Oh, S.-J.; Choi, J.-Y.; Kim, J. W. Chem Mater 2005, 17, 5057.
13. Zeng, Q. H.; Yu, A. B.; Lu, G. Q.; Paul, D. R. J Nanosci Nanotechnol 2005, 5, 1574.
14. Chang, J.-H.; Kim, S. J.; Job, Y. L. Polymer 2004, 45, 919.
15. Guan, G.-H.; Li, C.-C.; Zhang, D. J Appl Polym Sci 2005, 95, 1443.
16. Aht-Ong, D.; Benjapornthavee, H. International Conference on Nanosci and Nanotechnol, ICONN 2008, 2008, 1.
17. Wang, G.; Wang, O. J Polym Sci Part B: Polym Phys 2008, 46, 807.
18. Todorov, L. V.; Viana, J. C. J Appl Polym Sci 2007, 108, 1659.
19. Acierno, D.; Amendola, E.; Napolitano, G. Macromol Symp 2007, 247, 120.
20. Tharmapuram, S. R.; Jabarin, S. A. Adv Polym Technol 2003, 22, 137.
21. Jacobson, A. J Mater Sci Forum 1994, 152/153, 1.
22. Sun, L.; Boo, W. J.; Liu, J.; Tien, C. W.; Sue, H.- J.; Mullins, M. J.; Pham, H. Polym Eng Sci 2007, 47, 1708.
23. Wang, K.; Wang, L.; Wu, J.; Chen, L.; He, C. Langmuir 2005, 21, 3613.
24. Wolf, D.; Fuchs, A.; Wagenknecht, U.; Kretzschmar, B.; Jehnichen, D.; Haussler, L. Proceedings of Eurofiller'99, Lyon-Villeurbanne, France, 1999; p 6.

25. Chen, B.; Evans, J. Polym Int 2005, 54, 807.
26. Nadeau, P.; Tait, J. Clay Miner 1984, 19, 67.
27. Calcagno, C. I. W.; Mariani, C. M.; Teixeira, S. R.; Mauler, R. S. Polymer 2007, 48, 966.
28. Calcagno, C. I. W.; Mariani, C. M.; Teixeira, S. R. J Appl Polym Sci 2009, 111, 29.
29. Ou, C. F.; Ho, M. T.; Lin, J. R. J Appl Polym Sci 2004, 91, 140.
30. Usuki, A.; Kojima, Y.; Kawasumi, M.; Okada, A. J Appl Polym Sci 1995, 55, 119.
31. Chen, B.; Evans, J. Scr Mater 2006, 54, 1581.
32. Giannelis, E. P. Adv Mater 1996, 8, 29.
33. Vlasveld, D. P. N.; Groenewold, J.; Bersee, H. E. N.; Mended, E.; Picken, S. J. Polymer 2005, 46, 6102.
34. Hwang, S. Y.; Lee, W. D.; Lim, J. S. J Polym Sci Part B: Polym Phys 2008, 46, 1022.
35. Kim, K. H.; Kim, K. H.; Hun, J. Macromol Res 2007, 15, 178.
36. Min, K. D.; Kim, M. Y.; Choi, K.-Y.; Lee, J. H. Polym Bull 2006, 57, 101.
37. Chang, J. H.; Park, D. K. Polym Bull 2001, 47, 191.
38. Frounchi, M.; Dourbash, A. Macromol Mater Eng 2008, 294, 68.